J MATER RES TECHNOL. 2019;8(2):1835–1848

Available online at www.sciencedirect.com

jmr&t Journal of Materials Research and Technology

www.jmrt.com.br

Original Article

Effects of geometry and hybrid ratio of steel and polyethylene fibers on the mechanical performance of ultra-high-performance fiber-reinforced cementitious composites

Min-Jae Kim[a], *Doo-Yeol Yoo*[a,*], *Young-Soo Yoon*[b,*]

[a] *Department of Architectural Engineering, Hanyang University, 222 Wangsimni-ro, Seongdong-gu, Seoul 04763, Republic of Korea*
[b] *School of Civil, Environmental and Architectural Engineering, Korea University, 145 Anam-ro, Seongbuk-gu, Seoul 02841, Republic of Korea*

ARTICLE INFO

Article history:
Received 27 July 2018
Accepted 11 January 2019
Available online 16 February 2019

Keywords:
UHPFRCC
Steel fiber
Polyethylene fiber
Fiber hybridization
Mechanical performance
Synergy effect

ABSTRACT

This study aims to examine the several factors influencing the efficiency of the hybridization of steel and polyethylene (PE) fibers in improving the compressive strength and tensile performance of ultra-high-performance fiber-reinforced cementitious composites (UHPFRCC). For the mechanical tests, three types of steel fibers (i.e., short straight steel (SS), medium-length straight steel (MS), and twisted steel (T) fibers) and four lengths of polyethylene (PE) fibers (i.e., 12 mm (SPE), 18 mm (MPE), 27 mm (LPE), and 36 mm (LLPE)) were hybridized. Each specimen included 2 vol.% of single or hybrid fibers, and the hybrid ratio was controlled by replacing 0.5% of the steel fibers with the same amount of PE fibers from 0 to 2%. Thus, a total of 7 single and 36 hybrid UHPFRCC specimens were fabricated. From the test results, it was found that the compressive strength decreased proportionally to the PE fiber content, but the decrease was more severe in hybrid specimens, including 1.5% PE fibers, than single fiber specimens, including 2.0% PE fibers. The tensile strength also decreased with an increase of PE fiber content, whereas strain capacity and energy absorption capacity per unit volume substantially improved with the inclusion of PE fibers. The SPE fibers showed the best hybridizing efficiency among PE fibers in improving the tensile strain capacity and energy absorption capacity of UHPFRCC, and the use of T fibers was the most effective in terms of cracking behavior.

* *Corresponding authors.*
E-mails: dyyoo@hanyang.ac.kr (D. Yoo), ysyoon@korea.ac.kr (Y. Yoon).
https://doi.org/10.1016/j.jmrt.2019.01.001

1. Introduction

Richard and Cheyrezy [1] first introduced reactive powder concrete (RPC) with only fine aggregates and high volume contents of micro straight steel fibers in the 1990s. After that, many researchers [2–7] have made efforts to improve the performance of RPC, also called ultra-high-performance fiber-reinforced cementitious composites (UHPFRCC), with better mechanical properties. UHPFRCC is comprised of fine powders, such as cement, silica fume, silica sand, and silica flour, and also includes a large amount of steel fibers to achieve a more homogeneous and denser micro-structure and strain-hardening behavior under tension [5,6]. In addition, it undergoes a high-temperature steam curing process and thus shows excellent compressive strength over 150 MPa and tensile strength over 8 MPa. However, this material still has some limitations for use in various construction applications because of its brittle tensile behavior, showing a lower strain capacity, normally below approximately 0.5%, relative to that of engineered cementitious composites (ECC).

Various studies [3,4,6,8–10] have been conducted for the purpose of improving the tensile strength and ductility of fiber-reinforced cementitious composites (FRCC). One of the most useful methods is to adjust the fiber-matrix interaction [4,6,8,9], and another is to hybridize steel and polymeric fibers [3,10]. Regarding the first method, Naaman et al. [8] developed Torex twisted fibers in the 1990s to obtain additional pullout resistance by the mechanical anchorage effect. This fiber type resulted in greater tensile performance in high-performance fiber-reinforced cementitious composites (HPFRCC). However, it was also recently reported that the superb mechanical anchorage induced deterioration and splitting cracks in the UHPFRCC matrix [4,6,9]. Yoo et al. [9] found that hooked-end and twisted steel fibers led to severe deterioration of the matrix, and even lower flexural strength and ductility were observed as compared to those of straight steel fibers. This was verified by observing unrecovered deformation of the hooked and twisted fibers after testing. Kim et al. [4] and Wille et al. [6] also similarly reported the high stress concentration and its influence on the local deterioration of the UHPFRCC matrix. In the meantime, ECC, which is another type of HPFRCC, was developed, and its performance was improved by a number of researchers [11–14]. ECC generally incorporates 2 vol.% polymeric fibers to enhance the tensile strength and ductility. Although ECC has comparatively lower compressive or tensile strengths of 30–50 MPa or 5–8 MPa, respectively, than those of UHPFRCC, it usually shows a much higher strain capacity over 4% [12]. Such an excellent tensile strain capacity was achieved by Li et al. [12], who tailored the fiber-matrix interaction by oiling polyvinyl alcohol (PVA) fibers, which could protect the fibers from being laminated or having a high stress concentration, obtained by strong frictional resistance from the matrix.

Kim et al. [10] and Yoo and Kim [3] examined the influence of the hybridization of steel and polyethylene (PE) fibers on the tensile behavior of UHPFRCC. Kim et al. [10] focused on twisted fibers hybridized with four lengths of PE fibers, while Yoo and Kim [3] focused on three types of steel fibers (i.e., short straight, medium-length straight, and twisted steel fibers), hybridized with only one length of PE fiber. The authors [3,10] found that the steel and PE fibers have different pull-out mechanisms and impacts on the matrix. Since the steel and PE fibers have different physical and chemical properties, adjusting their hybridization details, such as hybrid ratios and fiber properties, can result in substantial enhancement in the tensile performance of UHPFRCC. Therefore, it is still required to comprehensively examine the exact influences of the geometrical deformation, aspect ratio, and hybrid ratio of steel and polymeric fibers on the tensile performance of UHPFRCC in order to determine the optimum fiber hybridization, most greatly enhancing the strain and energy absorption capacities. In this study, three different types of steel fibers were thus hybridized with four types of PE fibers having different lengths for fabricating UHPFRCC at five replacement ratios from 0 to 2%. Moreover, the hybrid effects of the various steel and PE fibers on both the compressive and tensile performances of UHPFRCC were synthetically evaluated in order to determine the optimum fiber types and replacement ratios.

2. Experimental program

2.1. *Materials and specimen fabrication*

The mixture proportion of the ultra-high-performance cement composite (UHPCC) matrix is tabulated in Table 1. First, it should be noted that coarse aggregate was not included in the mix for improving its homogeneousness and fiber pullout resistance derived from the higher shrinkage of the mixture [15,16]. Type 1 Portland cement and silica fume (SF) with a diameter of approximately 0.2–0.3 μm were used as cementitious materials and other granular materials (i.e., silica sand with a diameter of 0.2–0.3 mm as a fine aggregate and silica flour with a diameter of less than 10 μm as a filler) were incorporated for better physical and mechanical properties. The chemical and physical properties of the cement and SF are summarized in Table 2. The cement contains 61.3% CaO and 21.0% SiO_2, while the silica fume contains 96% SiO_2. A very low water to binder (W/B) ratio of 0.2 was adopted to achieve a higher strength matrix, and polycarboxylate superplasticizer (SP), consisting of 30% solid and 70% water, was used to assure a proper workability. In this study, the amount of SP was flexibly controlled to obtain the proper flowability according to the volume content of PE fibers, because they significantly reduced the flowability of the fresh UHPCC mixture.

Three types of steel fibers, short straight (SS), medium straight (MS), and twisted (T) fibers with lengths of 13, 19.5, and 30 mm and diameters of 0.2, 0.2, and 0.3 mm, respectively, were used. Subsequently, four types of PE fibers with lengths of 12, 18, 27, and 36 mm and the same diameter of 30 μm were adopted, and these fibers are denoted as SPE, MPE, LPE, and LLPE fibers, respectively. Their physical and mechanical properties are summarized in Table 3. The tensile strengths of SS (or MS) and T fibers were 2428 and 2788 MPa, respectively, and their elastic modulus was found to be 200 GPa, while the PE fibers had a tensile strength of approximately 3030 MPa and an elastic modulus of 88 GPa. These steel and PE fibers were used in both single and hybrid forms. The total fiber volume content was fixed at 2.0% for all the specimens, and the replacement ratio of steel fibers increased at intervals of 0.5%. For instance,

Table 1 – Mixture proportion of UHPCC.

W/B[b]	Unit weight (kg/m^3)					
	Water	Cement	Silica fume	Silica sand	Silica flour	Superplasticizer[a]
0.2	160.3	788.5	197.1	867.4	236.6	52.6

[a] Superplasticizer includes 30% solid (=15.8 kg/m^3) and 70% water (=36.8 kg/m^3).
[b] W/B is calculated by dividing total water content (160.3 kg/m^3 + 36.8 kg/m^3) by total amount of binder (788.5 kg/m^3 + 197.1 kg/m^3).

Table 2 – Compositions and physical properties of cement and silica fume.

Composition % (mass)	Cement[a]	Silica fume
CaO	61.33	0.38
Al_2O_3	6.40	0.25
SiO_2	21.01	96.00
Fe_2O_3	3.12	0.12
MgO	3.02	0.10
SO_3	2.30	–
Specific surface area (cm^2/g)	3413	200,000
Density (g/cm^3)	3.15	2.10

[a] Type 1 Portland cement.

Table 3 – Physical and mechanical properties of steel and PE fibers.

Name	L_f (mm)	d_f (mm)	Aspect ratio (L_f/d_f)	Density (g/cm^3)	f_t (MPa)	E_f (GPa)
SS	13	0.2	65.0	7.9	2788	200
MS	19.5	0.2	97.5	7.9	2428	200
T	30	0.30	100	7.9	2428	200
SPE	12	0.03	400	0.97	3030	88
MPE	18	0.03	600	0.97	3030	88
LPE	27	0.03	900	0.97	3030	88
LLPE	36	0.03	1200	0.97	3030	88

Note: d_f, fiber diameter; l_f, fiber length; f_t, tensile strength of fiber; E_f, elastic modulus of fiber; SS, short straight steel fiber; MS, medium-length straight steel fiber; T, twisted steel fiber; SPE–LLPE, polyethylene fibers with four different aspect ratios.

the SS and PE fibers are hybridized to be SS2.0, SS1.5–PE0.5, SS1.0–PE1.0, SS0.5–PE1.5, and PE2.0. Herein, the letters SS and PE denote fiber types, and the subsequent numbers denote their volume fraction. Thus, each type of steel fibers has five replacement ratios from 0 to 2% using PE fibers with four different lengths.

The UHPFRCC mixture was fabricated according to the following steps: (1) dry materials, including cement, silica fume, silica flour, and silica sand, were dry-mixed for 10 min, (2) water premixed with SP was poured into the mixture and it was mixed for an additional 10 min until it achieved self-consolidating capacity, and (3) the steel fibers were carefully added into the mixture and mixed for the last 5 min to assure their fine dispersion. In particular, the PE fibers were premixed with the dry materials to obtain a better distribution in the mixture. Once the mixture was prepared, it was cast into molds and sealed with a plastic sheet for prevention of drastic drying. The fabricated specimens went through 3 days of steam curing at 90° after 1 day of air dry curing at room temperature. The specimens were located in a laboratory at room temperature until the testing date after finishing the steam curing.

2.2. *Compressive strength measurement*

In this study, two types of test specimens were used in order to investigate the effect of the specimen's shape on the compressive strength. For this, according to ASTM C 109 [17] and ASTM C 39 [18], 50 mm cubes and ø100 mm × 200 mm sized cylinders were fabricated and tested, respectively. The top and bottom sides of the cylindrical specimens were ground using a diamond blade to minimize the eccentric effect, and the cubic specimens were tested by rotating 90° from the casting surface for the identical purpose. A universal testing machine (UTM) with a load capacity of 3000 kN was used for applying a uniaxial compressive load, and the loading rate was controlled at 0.1 mm/min.

2.3. *Direct tensile test*

The uniaxial direct tensile tests were conducted as per JSCE recommendation [19]. Details of the test setup and specimens are illustrated in Fig. 1a and b, respectively. A UTM with a maximum load capacity of 300 kN was used for the tests, and the loading rate applied was 0.4 mm/min. Two linear variable

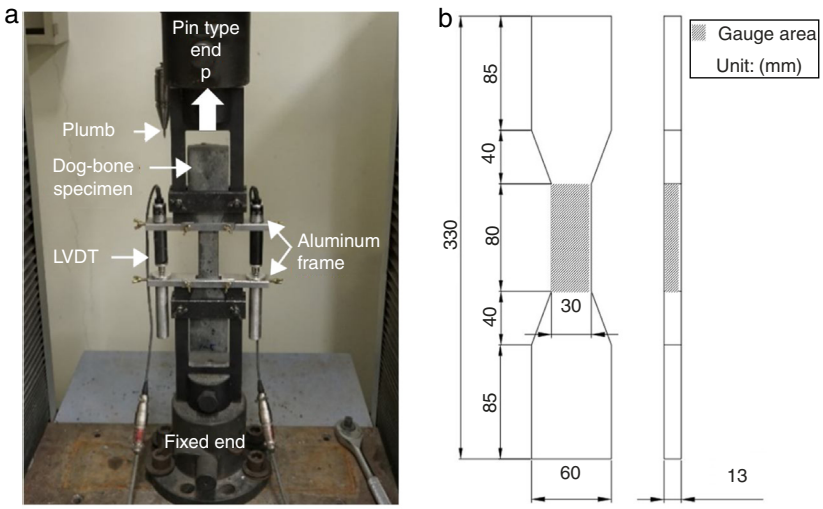

Fig. 1 – Direct tensile test setup: (a) picture and (b) details of specimen geometry.

displacement transformers (LVDTs) were used to measure the elongation of dog-bone specimens within the gauge length of 80 mm. The measured tensile load and elongation were transformed to the tensile stress and strain in the gauge region, respectively, to obtain the tensile stress-strain curve. The dog-bone specimen has a cross-sectional area of $13 \times 30\,mm^2$, as shown in Fig. 1b. A plumb was used for specimen alignment, and a pin-fixed type end condition was applied for minimizing the eccentric effect. In order to visualize microcracks clearly, polyurethane was sprayed on the surface of the specimens two or three times after the steam curing process. After completing the tensile test, ethanol was sprayed on the surface of the specimens coated with polyurethane for detecting microcracks with the naked eye.

3. Test results and analysis

3.1. *Comparison of compressive strength according to the aspect of the test specimen*

The compressive strength test results obtained from both the cubic and cylindrical specimens are given in Fig. 2. Previous studies [20,21] have reported that the compressive strength depends on the size and aspect of the concrete specimens tested. Graybeal and Davis [22] and del Viso et al. [20] examined the size effects on the compressive strength by using several types of cubic and cylindrical specimens, and their test results showed that the 50-mm cubic specimens generally provided 0–16% higher compressive strengths than the cylindrical specimens ($\varphi 100\,mm \times 200\,mm$). The test results of this study similarly revealed that the cubic specimens had 0–41% higher compressive strengths than those of the cylindrical specimens in general. Fig. 3 shows relationships between the compressive strengths obtained from all of the cubic and cylindrical specimens for each variable, and the data was fitted with a linear function: $y = 0.629x + 67.6$, with a determination coefficient, R^2, of 0.544. Herein, y indicates the compressive strength of a cubic specimen and x denotes the compressive strength of a cylindrical specimen. According to this fitting line, the cubic specimens showed higher compressive strengths than the cylindrical specimens at compressive strength values below approximately 160 MPa, but the difference was reduced as the values increased up to 200 MPa.

Based on the data analyses of cylindrical specimens, several important findings were observed, as follows. The effect of fiber type is less influential on the compressive properties than the tensile properties of UHPFRCC [21]. Consistently, the three types of single steel fiber-reinforced specimens (i.e., SS2.0, MS2.0, and T2.0) did not provide discernable differences in the compressive strength, whereas the PE fibers greatly decreased the compressive strength of UHPFCC in proportion to their volume fraction, as shown in Fig. 2a. For example, the compressive strengths of the SS2.0, MS2.0, and T2.0 specimens incorporating 2 vol.% of steel fibers measured to be 187, 192, and 205 MPa, respectively, similar to previous studies [9,23]. The compressive strength, however, started decreasing as the PE fiber portion increased. When 0.5 vol.% of SS, MS, and T fibers were replaced with PE fibers, the average compressive strength decreased to 164, 131, and 186 MPa, respectively. Such decreasing trends were maintained until the PE fiber volume fraction increased up to 1.5%. Subsequently, the average compressive strengths of specimens including 1.0 vol.% of SS, MS, and T fibers and 1.0 vol.% of PE fibers were found to be approximately 160, 116, and 166 MPa, respectively, while those of specimens including 0.5 vol.% of SS, MS, and T fibers and 1.5 vol.% of PE fibers were approximately 123, 115, and 111 MPa, respectively. The great decrease of compressive strength by increasing the replacement ratio might be caused by the balling effect of the PE fibers having much higher aspect ratios. Polymeric fibers normally have very high aspect ratios and a tendency to aggregate together in cement matrix as compared to those of steel fibers as shown in Fig. 4a. The agglomerated PE fibers thus act as unintended pores leading

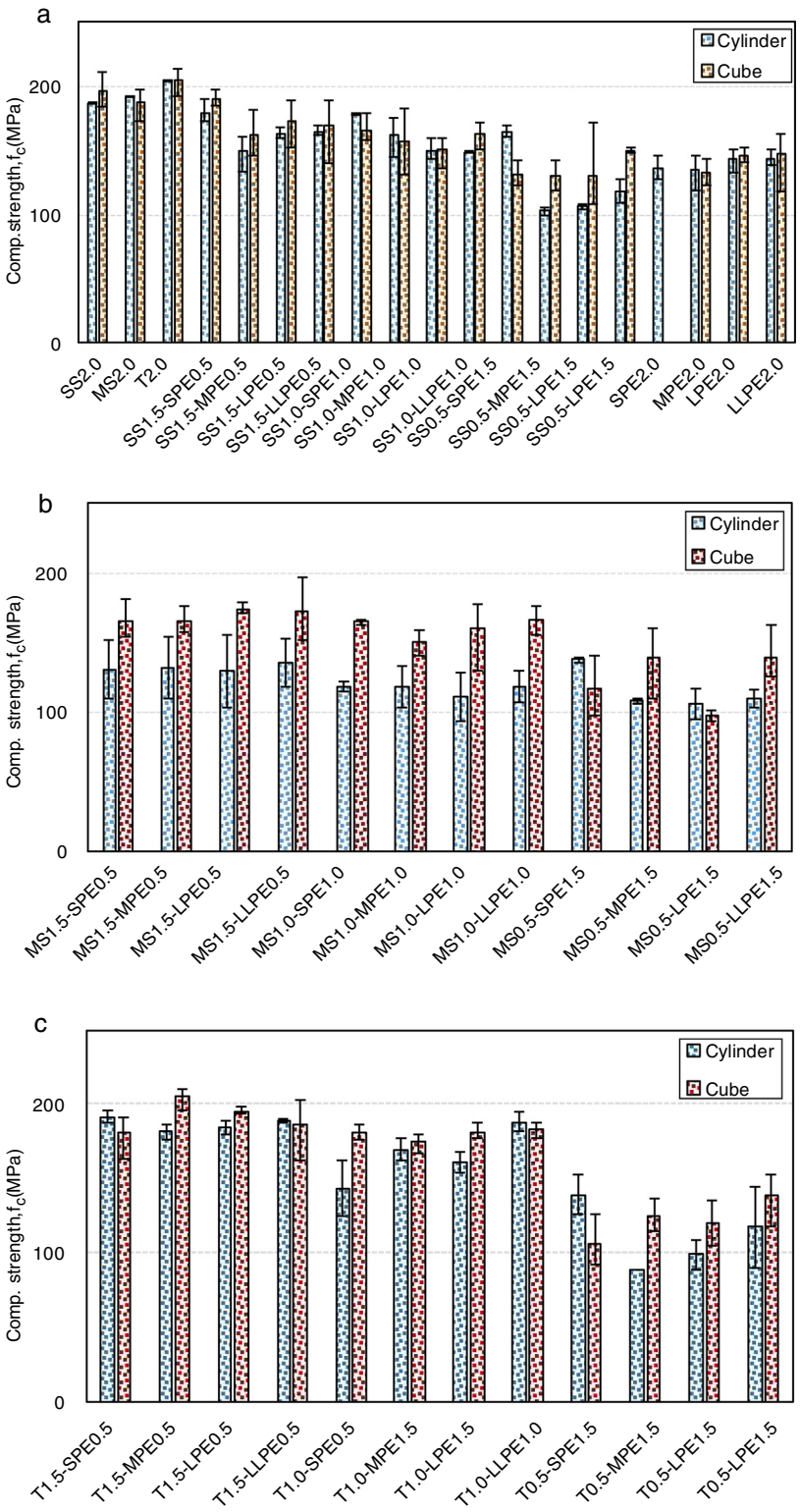

Fig. 2 – Summary of compressive strengths of (a) SS-PE series, (b) MS-PE series, and (c) T-PE series.

to a weaker load transferring system and lower strengths under compression [13,24]. The lowest compressive strengths were obtained in the specimens with 1.5 vol.% steel fibers and 0.5 vol.% PE fibers, and these values were even lower than the compressive strengths of the PE2.0 series, which is approximately 140 MPa on average. Based on this observation, it can be noted that the steel and PE fibers have detrimental mutual influence on the fiber dispersion or alignment, deriving vulnerable zones that decrease the compressive strength of UHPFRCC.

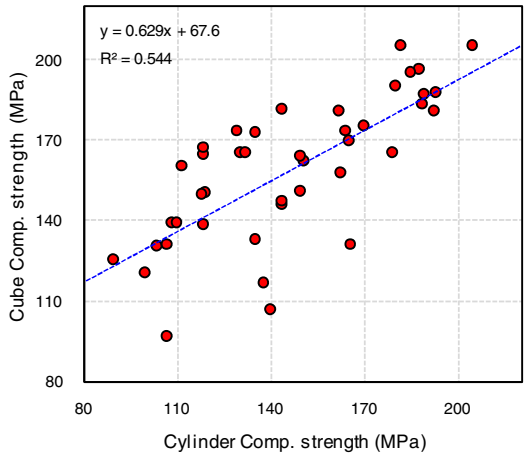

Fig. 3 – Relationship between compressive strengths measured from cubic and cylindrical specimens.

3.2. *Effect of steel and PE fiber hybridization on the tensile performance of UHPFRCC*

The tensile stress-strain curves of all tested specimens are summarized in Figs. 5–7 according to the steel fiber type. The tensile strength, f_t, in MPa, strain capacity, ε_t, in %, and energy absorption capacity up to the peak point, called the *g*-value, in kJ/m^3 are also given in Fig. 8a, b, and c, respectively.

3.2.1. *Tensile stress versus strain response*

Figs. 5–7 show the tensile stress and strain curves of single and hybrid UHPFRCC specimens, organized by reinforcement ratios. From Fig. 5a showing the stress and strain responses of the single steel fiber-reinforced specimens, the post-cracking stiffness of the MS2.0 specimen was the highest, followed by the SS2.0 and T2.0 specimens. The tensile stress of the MS2.0 specimen increased to its peak point and provided a strain capacity of 0.89%, while the SS2.0 and T2.0 specimens showed smaller strain capacities of 0.57% and 0.52%, respectively. The post-peak ductility of the T2.0 specimen was the lowest among the three different specimens, and this resulted from the matrix deterioration due to the untwisting torque of the T fiber mentioned above [9]. The post-cracking stiffness was reduced as the amount of PE fibers increased. Although this effect was insignificant at the replacement ratios of 0.5 and 1.0%, as shown in Figs. 5 and 6, it became obvious at the replacement ratio of 1.5%, and thus, the strain capacity greatly increased. In addition, the post-cracking stiffness generally decreased as longer PE fibers were used. In Figs. 5–7, it is seen that the post-cracking stiffness of the specimens including LPE or LLPE fibers was lower than the specimens with SPE or MPE fibers, except for the SS0.5–PE1.5 series (Fig. 7a). In this series, the tensile stresses of the specimens with LPE or LLPE fibers more drastically increased and decreased, compared to those with SPE or MPE fibers. In the meantime, the post-cracking stiffness did not vary depending on the length of the PE fibers in the PE2.0 series, as shown in Fig. 7d.

Overall, the single steel fiber specimens showed smooth stress and strain curves, but as the steel fibers were replaced with the PE fibers, the shape of the curves began fluctuating, as shown in Figs. 5–7. For the hybrid fiber specimens, the fluctuation persisted longer at higher replacement ratios. This data fluctuation was derived from the fact that the PE fibers are provided with a strong frictional pullout resistance that is longer than the steel fibers from the matrix. In a previous study [23], it was found that after debonding process steel fibers are provided with weaker and shorter frictional resistance by cement matrix than the PE fibers because they have a much higher surface hardness and mash the matrix particles at the interface as they are pulled out. On the other hand, the PE fibers have soft surface texture and generally get much stronger and longer-lasting frictional resistance from the same cement matrix. Fig. 4b and c show optical microscopic images taken during tensile tests which present influence of steel and PE fiber pullout on cement matrix. Herein, it was observed that the T fibers with twisted geometry split and weaken the nearby matrix, whereas the matrix nearby several PE fibers were just teared off because of persistent and strong frictional pullout resistance. In the meantime, once the tensile stress of the hybrid specimens began decreasing, the stress-strain curve gradually became smooth, similar to that of the single steel fiber specimens, and this led to crack localization. The steel fibers have comparatively stiffer surface conditions than matrix particles, so they were not provided with the persisting strong frictional pullout resistance. In addition, Li and Leung [25] reported that if fibers have too strong of an interface with the matrix, the complementary energy becomes low and each crack surface is expanded rather than being flat, resulting in tension softening behavior. In the same vein, the steel fibers have a strong chemical bond with the matrix, and this resulted in a low complementary energy, earlier tension softening behavior, and smoother stress–strain response than the specimens including the PE fibers.

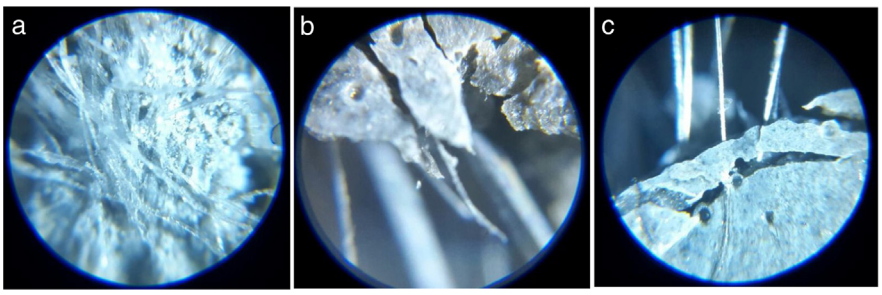

Fig. 4 – Optical microscopic images (a) PE fiber balling, (b) split matrix by pullout of T fiber, and (c) matrix tearing off by pullout of PE fibers.

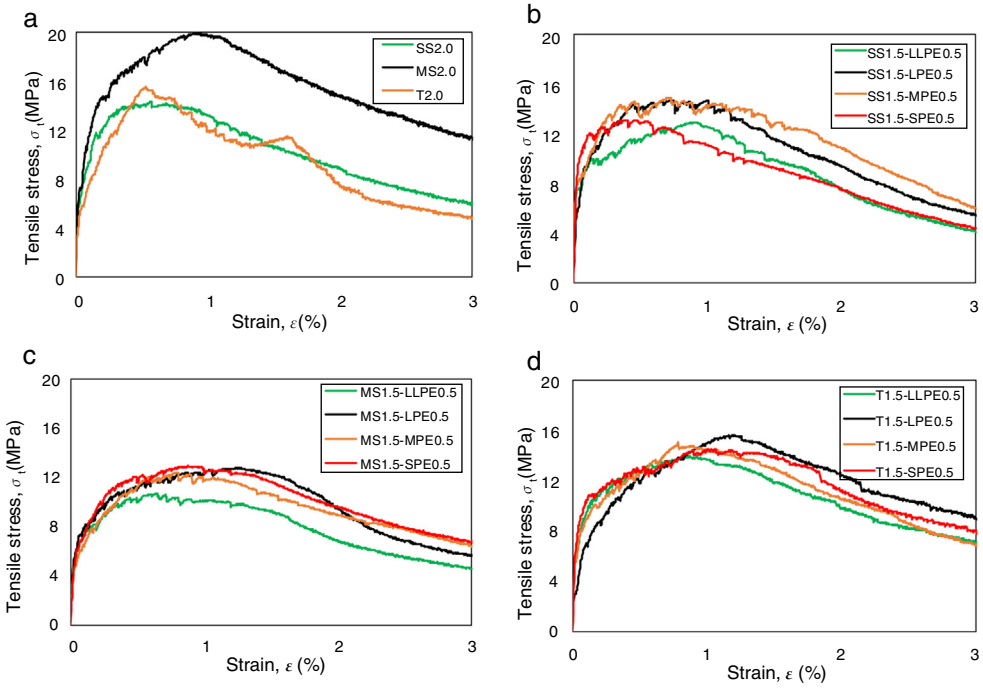

Fig. 5 – Tensile stress versus strain curves for (a) steel fibers with 2%, (b) SS1.5–PE0.5, (c) MS1.5–PE0.5, and (d) T1.5–PE0.5.

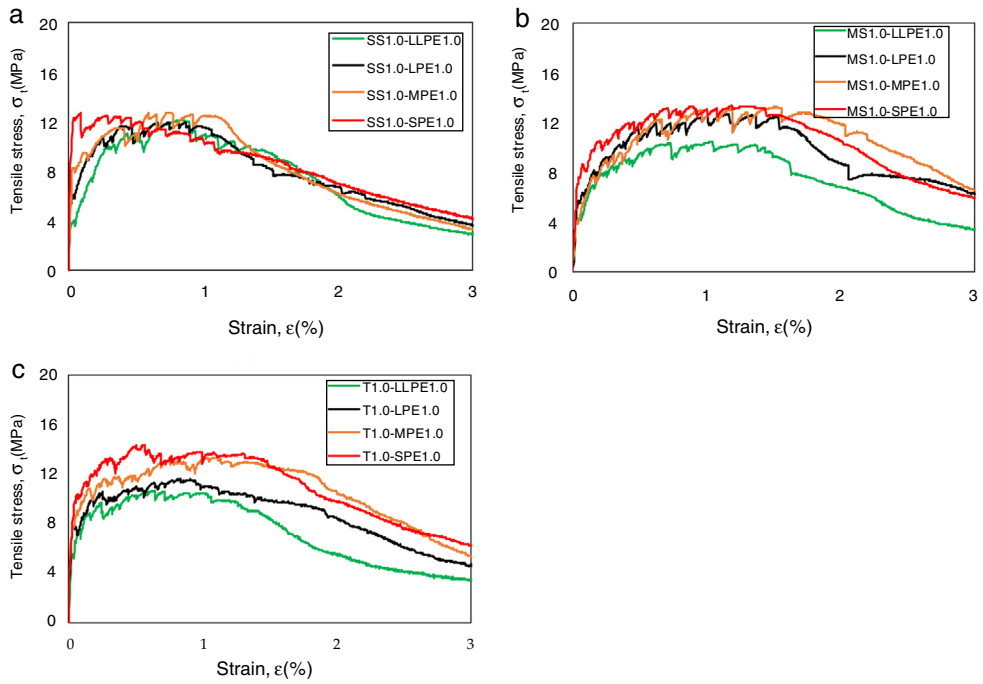

Fig. 6 – Tensile stress versus strain curves for (a) SS1.0–PE1.0, (b) MS1.0–PE1.0, and (c) T1.0–PE1.0.

Comparing the stress–strain responses of the PE2.0 and hybrid series revealed interesting findings, as follows. The SPE fibers showed the lowest reinforcing efficiency in the PE2.0 series but the highest reinforcing efficiency at the replacement ratio of 1.5%, as shown in Fig. 7d. In the PE2.0 series, the tensile strength, strain capacity, and fluctuating amplitude of the SPE2.0 specimen were the lowest, but the hybrid specimens with 1.5% SPE fibers resulted in the highest tensile strength, strain capacity, and moderate fluctuating amplitude. This indicates that the 0.5% steel fibers and 1.5% SPE fibers performed well-divided roles at the crack surfaces. While the 0.5% steel fibers contributed to sustaining a larger

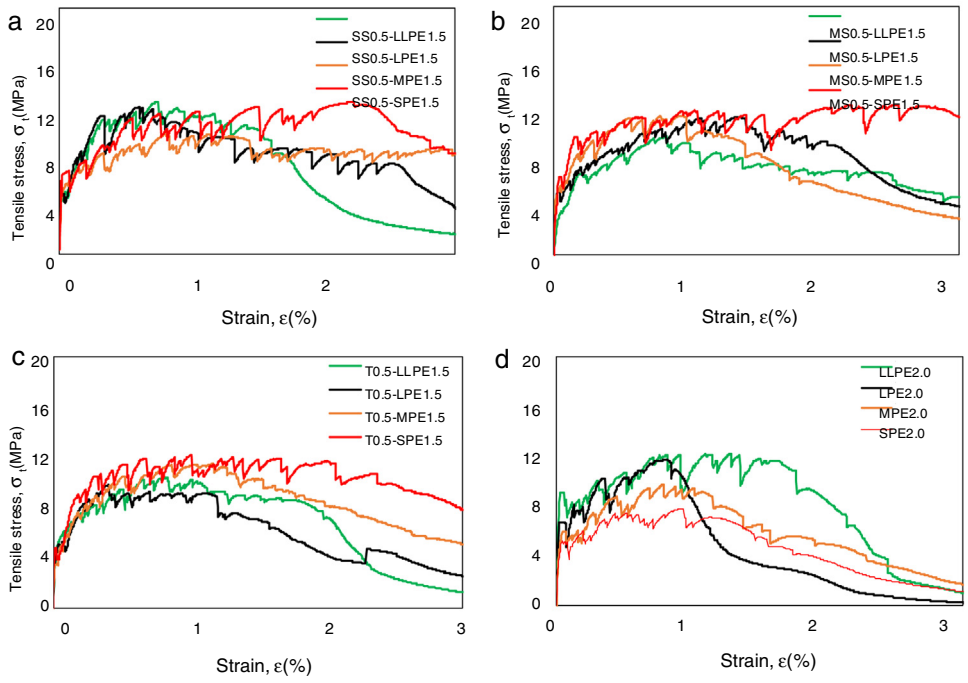

Fig. 7 – Tensile stress versus strain curves for (a) SS0.5–PE1.5, (b) MS0.5–PE1.5, (c) T0.5–PE1.5, and (d) PE2.0.

tensile force with a minor slip due to the strong fiber-matrix interface, the 1.5% SPE fibers contributed to reducing the post-cracking stiffness and resisting the tensile stress longer, which improved the strain-hardening property. However, the performance enhancement generally lessened as the length of the PE fibers increased at the replacement ratios of 1.0% or 1.5%, whereas the effect of the PE fiber length was minor at the replacement ratio of 0.5%, except for the specimens including SS fibers.

3.2.2. *Tensile strength*

As given in Fig. 8a, the tensile strength decreased with an increase in PE fiber content in general, regardless of the steel fiber type and aspect ratio of the PE fiber. This is similar to the results of compressive strength in Fig. 2. The SS2.0, MS2.0, and T2.0 specimens showed tensile strengths of approximately 14.4, 19.5, and 15.5 MPa, respectively, similar to a previous study [15]. Using the MS fiber with a length of 19.5 mm was more effective in enhancing the tensile strength of UHPFRCC than using the SS and T fibers. This is mainly affected by two factors: (1) the fiber length and aspect ratio influencing efficiency of fiber dispersion and orientation, and expected pullout length ratio, group reduction factor associated with the number of fibers pulling-out per unit area, snubbing coefficient, (2) the mechanical anchorage effect of the T fiber causing splitting cracks in the nearby matrix [3,5,9,24,26]. In previous research, it was also found that straight steel fibers with aspect ratios of 97.5 and 100 were discernably more effective in enhancing tensile strength of UHPCC than the one with an aspect ratio of 67.5. Meanwhile, the T fiber provides additional pullout resistance by its untwisting moment, but this effect has a tendency to produce general splitting cracks in the matrix, aggravating the resistance to fiber pullout [27]. Thus, the T2.0 specimen showed 15.5 MPa of tensile strength, which was higher than that of the SS2.0 specimen but lower than that of the MS2.0 specimen.

The tensile strengths were reduced in proportion to the replacement ratio of the steel fibers to the PE fibers. The average tensile strength of the SS2.0, MS2.0, and T2.0 specimens decreased to 13.9 (1.0), 12.2 (1.0), and 14.9 (0.7) MPa by replacing 0.5% of steel fibers with the PE fibers, to 12.8 (0.7), 12.4 (1.4), and 12.4 (1.7) MPa with 1.0% replacement, and to 11.6 (1.3), 11.1 (1.0), and 10.9 (1.1) MPa with 1.5% replacement, respectively, on average for all types of PE fibers. The values in parentheses indicate the standard deviation among the four test variables with different aspect ratios of PE fibers. These results denote that the steel fibers are more efficient to improve the tensile strength of UHPFRCC than the PE fibers in both the single and hybrid forms.

At the same replacement ratio, the tensile strength of the UHPFRCC specimens decreased slightly when the longer PE fibers were used, except for the specimens incorporating the SS fibers. It was also found that this deterioration became more obvious at the higher replacement ratio. For the series of MS1.5–PE0.5 fibers, the tensile strength decreased as much as 17.1% (from 12.9 to 10.7 MPa) as the PE fiber length increased from 12 mm (SPE) to 36 mm (LLPE). This decreasing ratio according to an increase in the PE fiber length for the series of MS1.0–PE1.0 and MS0.5–PE1.5 increased to 21.8% (from 13.3 to 10.4 MPa) and 20.7% (from 12.1 to 9.6 MPa), respectively. The T–PE hybrid series also showed similar trends: the tensile strengths of the T1.5–PE0.5, T1.0–PE1.0, and T0.5–PE1.5 series were reduced by 7.9%, 26.6%, and 16.4%, respectively, according to the increase of PE fiber length from 12 to 36 mm. These values were inconsistent with the results of the single PE2.0 specimens: the tensile strength proportionally increased

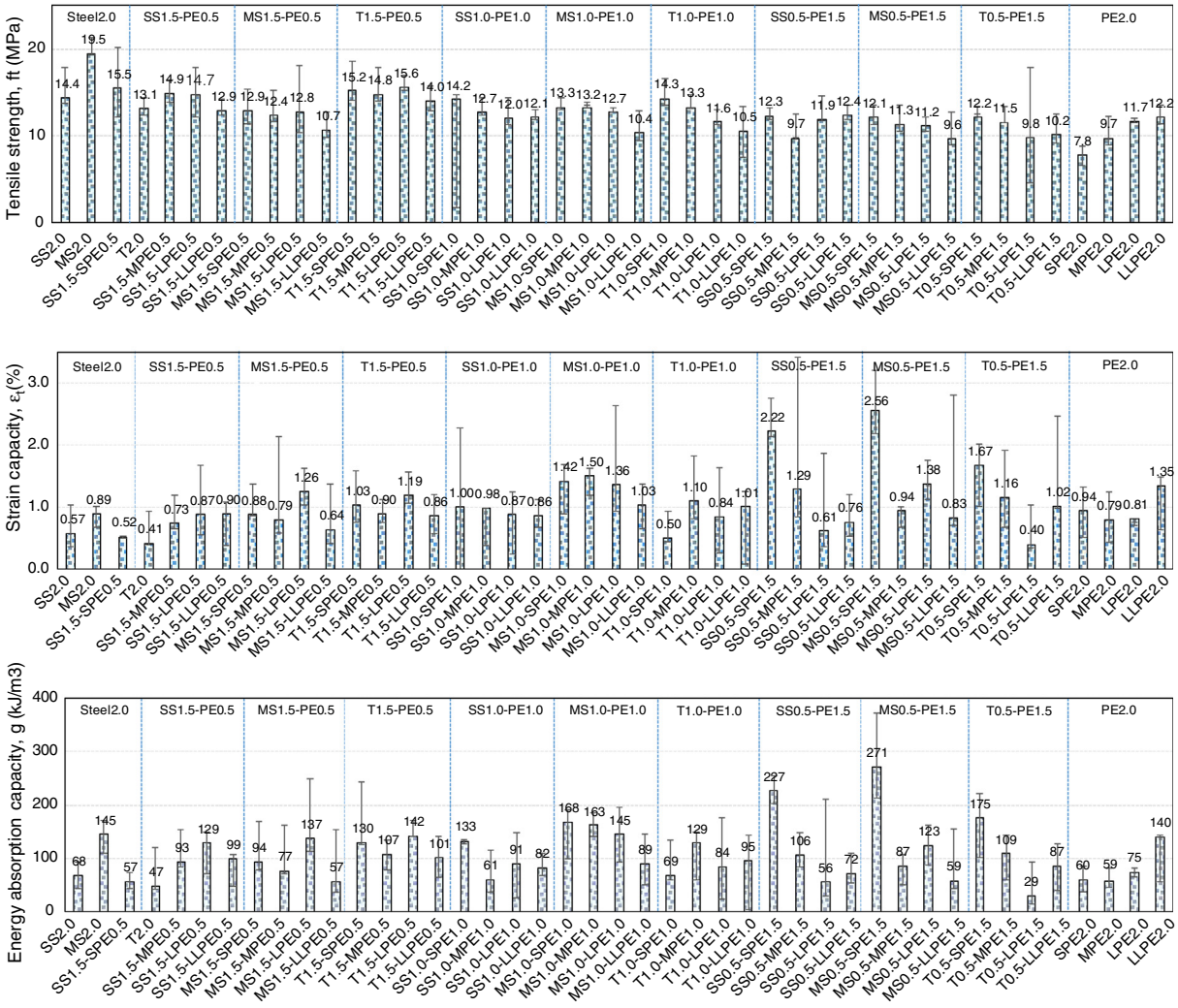

Fig. 8 – Summary of (a) tensile strength, (b) strain-capacity, and (c) energy absorption capacity.

from 7.8 to 12.2 MPa as the fiber length increased from 12 to 36 mm. In the meantime, the specimens including the SS fibers did not show considerable strength reduction depending on the length of hybridized PE fibers. The tensile strengths of the specimens with SS fibers and PE fibers at the replacement ratios of 0.5, 1.0, and 1.5% were found to be approximately 12.9–14.9, 12.0–12.7, and 9.7–12.4 MPa, respectively. The value of 9.7 MPa was the tensile strength of the SS0.5–MPE1.5 specimen, while that of the SS0.5–LLPE1.5 specimen was 12.4 MPa, which was 0.1 MPa higher than that of the SS0.5–SPE1.5 specimen. In addition, the increasing trend of the tensile strengths of SS0.5–PE1.5 series including MPE, LPE, and LLPE fibers was very similar to that of the PE2.0 series, as shown in Fig. 8a. In summary, it was found that the PE fiber length did not affect the tensile strength of the specimens including the SS fibers, whereas it clearly deteriorated that of the specimens including the MS and T fibers. Therefore, it can be noted that for the steel and PE fiber hybrid UHPFRCC, there is significant detrimental influence of longer lengths of PE fibers when they were hybridized with steel fibers with lengths over 19.5 mm.

3.2.3. *Strain capacity*

Fig. 8b shows that the strain capacities of the SS2.0, MS2.0, and T2.0 specimens were measured to be 0.57%, 0.89%, and 0.52%, respectively. Although the T fiber had the longest length and highest aspect ratio of 30 mm and 100, respectively, the T2.0 specimen showed the lowest strain capacity value at 0.52%. It was reported by previous studies [9,23,28] that longer steel fibers achieved superior ductile tensile or flexural behavior. However, the T fiber deteriorated the matrix by its untwisting torque, so that its pullout resistance from the matrix diminished earlier [6]. Therefore, the full bond strength of the T fiber could not be obtained from the direct tensile tests. It was obvious that the strain capacity greatly improved as a portion of the steel fibers was replaced with the PE fibers. This is caused by the different pullout properties derived from the different geometrical and physical conditions of the steel and PE fibers. When fibers are debonded from the cement matrix, fine matrix particles are detached and stacked up at the interface and provide frictional resistance to the pullout of fibers. The steel fibers have a much harder surface condition than

the cementitious particles at the interface and a high elastic modulus of 200 GPa, and thus, they tend to crush the particles at the interface and are easily pulled out with minor surface stretching [10]. In addition, strong chemical bonding between the steel fiber and cement matrix caused the matrix to be damaged during the debonding process. Alternatively, the PE fibers have a smaller diameter of 30 μm, tender surface texture, and very weak chemical bonding with the matrix [29], thus the matrix is less deteriorated during PE fiber pullout compared to that of steel fiber. In accordance with a previous study [29], the complementary energy, obtained from the stress and crack opening displacement curve, decreases with stronger chemical bonding since it raises the starting point of fiber bridging stress. The strain-hardening and multiple micro-cracking behaviors become more obvious in the FRC with higher complementary energy, so that the PE fiber is more effective in providing steady state crack growth and an obvious strain-hardening response with higher strain capacity than its counterpart (i.e., steel fibers). In addition, the PE fibers are provided with strong and continuous frictional resistance from the cement particles at the interface due to its softer surface condition, and this resulted in higher strain capacities of specimens including both the steel and PE fibers than that of the single steel fiber specimens.

The strain capacity of UHPFRCC reinforced with steel fibers significantly increased in proportion to the PE fiber hybrid ratio. The strain capacities of the SS2.0, MS2.0, and T2.0 specimens clearly increased to 0.73% (0.224), 0.89% (0.264), and 1.00% (0.149), respectively, when 0.5% of each type of steel fiber was replaced with the PE fibers on average. These values increased again to 0.93% (0.074), 1.33% (0.206), and 0.86% (0.265) at the 1.0% replacement ratio and 1.22% (0.728), 1.43% (0.792), and 1.06% (0.521) at the 1.5% replacement ratio on average, respectively. Herein, it can be seen that the standard deviation depending on the length of PE fibers increased as their content increases since the strain capacity largely decreased with an increase of PE fiber length when its hybrid ratio exceeded 0.5%, as shown in Fig. 8b. For instance, the strain capacity of the specimens including 1.0% of the SS and MS fibers and 1.0% of SPE fibers were measured to be 1.00% and 1.42%, respectively, and these values decreased to 0.86% and 1.03% as the length of the PE fibers increased to 36 mm (LLPE). This trend became clearer as the replacement ratio increased to 1.5%. For example, the strain capacities of the SS0.5–SPE1.5, MS0.5–SPE1.5, and T0.5–SPE1.5 specimens measured discernably high as 2.22%, 2.56%, and 1.67%, respectively, but largely decreased to 0.76%, 0.83%, and 1.02%, respectively, when the length of the PE fibers increased from 12 to 36 mm. However, at the replacement ratios of 0.5% and 2.0%, the detrimental effect of the PE fiber length on the strain capacity was not observed, and the strain capacities of the SS1.5–PE0.5 and PE2.0 series were even increased with increasing the PE fiber length from 12 to 36 mm, as shown in Fig. 8b.

There was a clear synergetic effect of hybridized steel and PE fibers, referring to the fact that the strain capacity of the hybrid UHPFRCC specimens was much higher than that of the single steel or PE fiber-reinforced specimens. The strain capacities of the single steel or PE fiber-reinforced specimens were found to be 0.52–0.89% or 0.79–1.35%, respectively, while those of the hybrid specimens with a replacement ratio of 1.5%, i.e., SS0.5–SPE1.5, MS0.5–SPE1.5, and T0.5–SPE1.5, were obtained as 2.22%, 2.56%, and 1.67%, respectively. This result is able to reinforce the assumptions, suggested by Nehdi and Ladanchuk [30] and Yao et al. [31], that the steel and PE fibers with different geometrical, physical, and mechanical properties affect the micromechanics of the cement composites. Furthermore, the possible explanation for this observation is as follows. The steel fibers tend to be pulled out easily after they are debonded from the cement matrix by mashing cement grains at the interface, because they have a higher surface hardness than the cement matrix. On the contrary, the PE fibers are resisted strongly and persistently by the matrix particles at the interface, leading to a more continuous increase in pullout resistance, and this can be the reason for the better efficiency of the PE fibers than the steel fibers in improving the tensile strain capacity of UHPFRCC.

3.2.4. *Energy absorption capacity*

In this study, the *g*-value, indicating the absorbed energy until the peak point of the tensile stress–strain curve and proposed by Wille et al. [27], was adopted. The calculated *g*-values for all the specimens are summarized in Fig. 8c. The single steel fiber reinforced specimens, i.e., the SS2.0, MS2.0, and T2.0 specimens, exhibited the *g*-values of 68.2, 144.9, and 56.6 kJ/m^3, respectively. The highest *g*-value was obtained in the MS2.0 specimen, because it provided a higher tensile strength and strain capacity of 19.5 MPa and 0.89%, respectively, than its counterparts. Alternatively, the SS fiber had a short length and the T fiber deteriorated the matrix, and thus, they could not enhance the tensile strength and strain capacity as much as the MS fiber, resulting in the lower energy absorption capacity.

Similar to the results of strain capacity, the g-value also increased with increasing replacement ratio in general. At the replacement ratio of 0.5%, the *g*-values of the SS2.0, MS2.0, and T2.0 specimens were changed to 91.9 (33.8), 91.1 (34.2), and 119.9 (19.2) kJ/m^3, respectively. Subsequently, these values varied to 91.4 (30.1), 141.5 (36.1), and 94.2 (25.5) kJ/m^3 with the 1.0% replacement ratio and changed to 114.9 (77.3), 134.9 (94.4), and 100.0 (60.3) kJ/m^3 with the 1.5% replacement ratio, respectively. In addition, the *g*-value largely decreased as longer PE fibers were incorporated at 1.0% and 1.5% in the hybrid specimens in general, as shown in Fig. 8c. For the SS1.0–PE1.0, MS1.0–PE1.0, and T1.0–PE1.0 series, the *g*-values were found to be 132.5, 167.9, and 68.6 kJ/m^3, respectively, as the SPE fibers were used. Those values, however, varied to 81.8, 89.3, and 95.2 kJ/m^3, as the LLPE fibers were incorporated. The T1.0–MPE1.0 specimen also provided the *g*-value of 128.7 kJ/m^3, which was 33.5 kJ/m^3 higher than that of the T1.0–LLPE1.0 specimen, although that of the T1.0–SPE1.0 specimen was the smallest at 68.6 kJ/m^3. Furthermore, the SS0.5–SPE1.5, MS0.5–SPE1.5, and T0.5–SPE1.5 specimens absorbed the energy under tension, approximately 226.5, 270.9, and 175.0 kJ/m^3, respectively. However, these values also largely decreased to 71.9, 58.7, and 86.8 kJ/m^3 when the LLPE fibers were incorporated. At the replacement ratio of 0.5%, the LPE fibers showed the best efficiency in improving the energy absorption capacity, due to their higher tensile strength and strain capacity, as shown in Fig. 8. There were also no noticeable trends according to the length of the PE fibers on the *g*-value in the series with the replacement ratio of 0.5% (Fig. 8c).

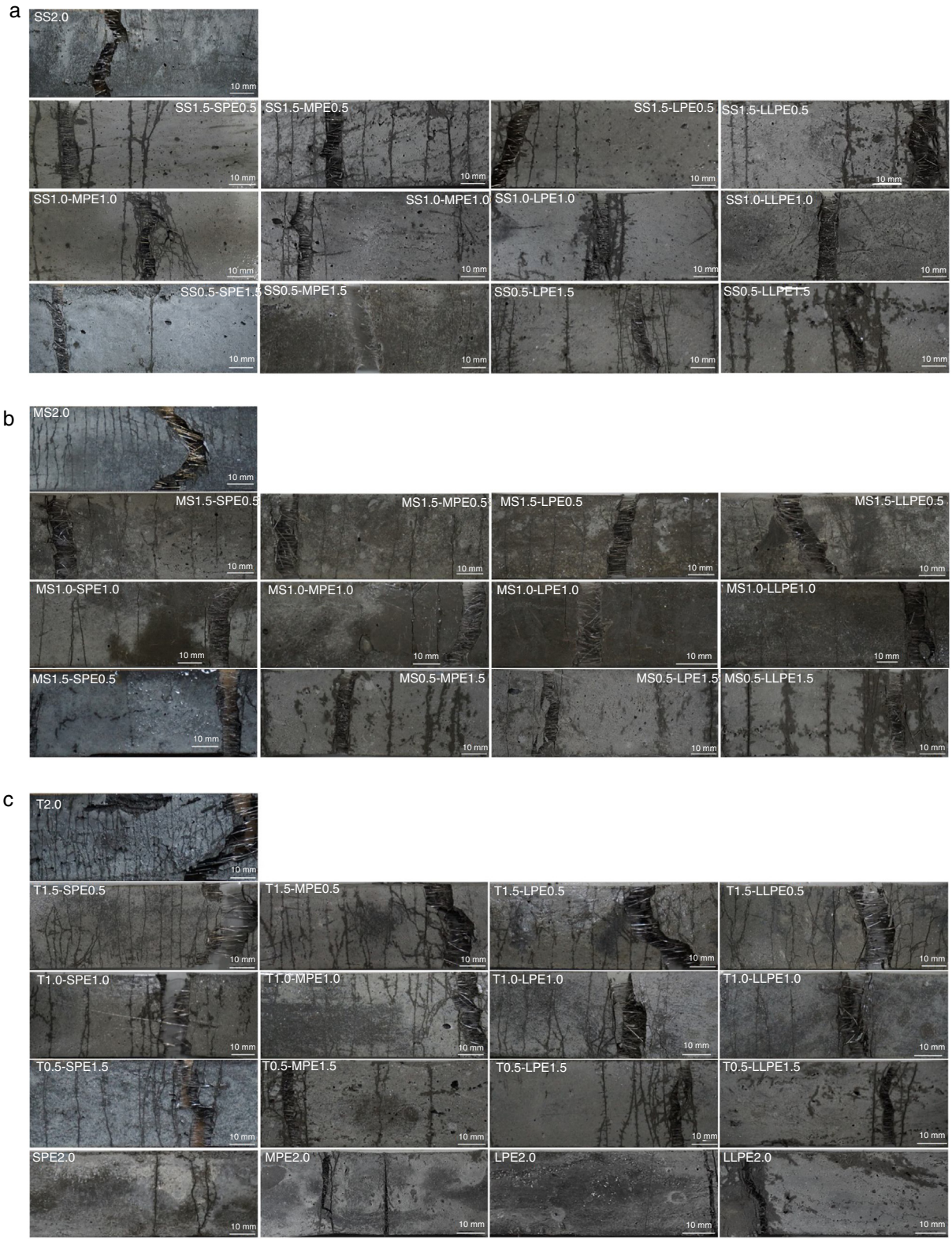

Fig. 9 – Cracking behaviors of (a) SS-PE series, (b) MS-PE series, and (c) T-PE series.

By comparing the *g*-values according to the replacement ratio and PE fiber length, we could obtain interesting results. Increasing the content of shorter PE fibers generally led to a great increase in the energy absorption capacity, while increasing the content of longer PE fibers resulted in the performance deterioration in the steel and PE fiber hybrid systems. Thus, the highest *g*-values were obtained for the specimens with steel and SPE fibers at the replacement

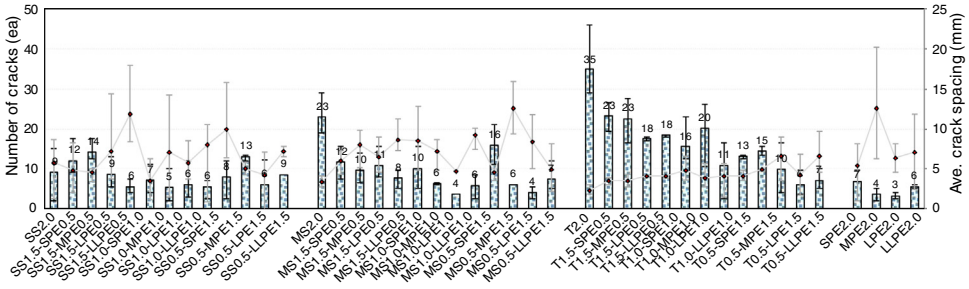

Fig. 10 – Summary of number of cracks and average crack spacing.

ratios of 1.0 and 1.5%. For example, the highest *g*-values were obtained in the SS1.0–SPE1.0, MS1.0–SPE1.0, and T1.0–MPE1.0 specimens as 132.5, 167.9, and 128.7 kJ/m^3 and in the SS0.5–SPE1.5, MS0.5–SPE1.5, and T0.5–SPE1.5 specimens as 226.5, 270.9, and 175.0 kJ/m^3, respectively. Most importantly, great synergistic effects were recorded in the energy absorption capacity of UHPFRCC. The highest *g*-values of all the steel and PE fiber hybrid specimens were found to be between 128.7 and 270.9 kJ/m^3, while the *g*-values of single steel or PE fiber reinforced specimens ranged between 57.0 and 144.9 kJ/m^3.

3.2.5. *Cracking behavior analysis*

Fig. 9 shows pictures of the crack patterns of all the tested specimens, while their cracking behaviors, including the number of cracks and average crack spacing, are given in Fig. 10. In general, the number of cracks exhibited opposite trends with the average crack spacing, similar to the results of Yoo et al. [28], because secondary microcracks are formed both outside and inside existing cracks. Therefore, the higher number of cracks resulted in a smaller average crack spacing. The number of cracks largely increased in the following order of steel fibers: SS, MS, and T fibers. The highest number of cracks was found to be 35 in the T2.0 specimen, approximately 289% and 52% higher than those of the MS2.0 and SS2.0 specimens, respectively. It is subsequently seen that the number of cracks was generally reduced with increasing both the volume content and length of the PE fibers for the cases including MS and T fibers, although there was some irregularity. For example, the number of cracks in the T2.0 specimen decreased to 23, 23, 18, and 18 as 0.5% T fibers were replaced with SPE, MPE, LPE, and LLPE fibers, respectively. The number of cracks continued decreasing to 16, 20, 11, and 13 when 1.0% T fibers were replaced and decreased to 15, 10, 6, and 7 when 1.5% T fibers were replaced with the PE fibers with various lengths, respectively. For the case of UHPFRCC including the SS fibers, however, this trend was not observed, and the number of cracks varied arbitrarily according to the volume content and length of the PE fibers. In addition, the highest number of cracks in the SS-fiber series was found to be 14, which is approximately 60% lower than that of the T2.0 specimen.

The cracking behavior was not obviously affected by the tensile strength and strain capacity. This means that the specimens with higher tensile strength and strain capacity do not always produce more microcracks. For instance, even though the T-fiber series did not provide better tensile performance than the SS- and MS-fiber series, they led to substantially higher numbers of cracks than their counterparts, which might be due to the additional mechanical anchorage of the T fiber through its entire embedment length. This could help to transfer the tensile stress and damage the surrounding matrix. Due to the superb bond strength, the inclined T fibers normally provide matrix spalling before reaching its ultimate strength. Therefore, the rougher surface of the localized cracks was observed in the T-fiber series as compared to the SS- and MS-fiber series, as shown in Fig. 9. For the cases of SS and MS fibers, the matrix spalling by inclination angle of fibers was minor relative to that of T fibers, owing to their lower pullout resistance, causing the smoother crack surfaces. This effect also became clearer when the PE fibers were included because they have no chemical bond with the matrix and mechanical anchorage effect, leading to significantly less damage on the surrounding matrix, as compared to the deformed steel fibers.

In general, with the replacement of steel fibers with the PE fibers, the number of cracks decreased, while the average crack spacing increased, as shown in Fig. 10. This trend became more obvious when a higher amount of steel fibers was replaced. Additionally, poorer cracking behaviors in terms of fewer microcracks and greater crack spacing were observed in the specimens with PE fibers than those with steel fibers. These observations were attributed to the different pullout mechanisms between them [3]. The steel fiber exhibits a very steep increase of pullout load with a minor slip in the full bonding and partial debonding zones, and this leads to effectively transferring the tensile load from the cracked surface to the surrounding matrix and forming more microcracks. However, the pullout load in the PE fibers increases more gradually along with partial delamination of the filament, so that the tensile load at the crack surface was not transferred to the surrounding matrix as efficiently as the steel fibers, resulting in the poorer cracking behaviors.

4. Conclusion

The hybrid effects of steel and PE fibers on the compressive strength and tensile performance of UHPFRCC were investigated. For this, three different types of steel fibers, i.e., SS, MS, and T fibers, and four types of PE fibers with different lengths, i.e., SPE, MPE, LPE, and LLPE fibers, were considered at the identical total volume fraction of 2%. From the test results and above discussions, the following conclusions can be drawn:

1. The compressive strength of UHPFRCC decreased in proportion to the volume fraction of PE fibers. In addition, 50-mm cubic specimens generally provided 0–41% higher compressive strengths than those of cylindrical specimens with a dimension of φ100 mm × 200 mm.
2. The MS fiber was most effective in enhancing the tensile strength of UHPFRCC among all the steel and PE fiber types used. The tensile strength decreased with an increase in the PE fiber content in general, regardless of the steel fiber type and PE fiber length. For the hybrid specimens, the tensile strength decreased as longer PE fibers were used at the identical replacement ratio, whereas that of the PE2.0 specimens increased in proportion to the length of the PE fibers.
3. The strain capacity of UHPFRCC reinforced with steel fibers significantly increased in proportion to its replacement ratio with PE fibers. The strain capacity greatly decreased with an increase in the PE fiber length when the replacement ratio exceeded 0.5%.
4. The *g*-values generally increased with increasing the amount of PE fibers, but they were reduced as longer PE fibers were incorporated at the replacement ratios of 1.0 and 1.5%. Increasing the amount of shorter PE fibers led to a great increase in the *g*-value, whereas increasing the amount of longer PE fibers resulted in performance deterioration in the hybrid specimens.
5. Synergetic effects of hybridized steel and PE fibers on enhancing the strain capacity and energy absorption capacity, referred as the *g*-value, of UHPFRCC were observed. Thus, the hybrid specimens provided much higher values of strain capacity and *g*-value than those of single steel and PE fiber-reinforced specimens.

Conflicts of interest

The authors declare no conflicts of interest.

Acknowledgements

This work was supported by the National Research Foundation of Korea (NRF) grant funded by the Korea government (MEST) (NRF-2016R1A2B3011392).

REFERENCES

[1] Richard P, Cheyrezy M. Composition of reactive powder concretes. Cem Concr Res 1995;25:1501–11.
[2] Banthia N, Trottier JF. Concrete reinforced with deformed steel fibers. 2. Toughness characterization. ACI Mater J 1995;92:146–54.
[3] Yoo DY, Kim MJ. High energy absorbent ultra-high-performance concrete with hybrid steel and polyethylene fibers. Constr Build Mater 2018 [in preparation].
[4] Kim DJ, Naaman AE, El-Tawil S. High performance fiber reinforced cement composites with innovative slip hardending twisted steel fibers. Int J Concr Struct Mater 2009;3:119–26.
[5] Naaman AE. Toughness, ductility, surface energy and deflection-hardening FRC composites. Proc JCI Int Work Ductile Fiber Reinf Cem Compos Appl Eval 2002:33–57.
[6] Wille K, Kim DJ, Naaman AE. Strain-hardening UHP-FRC with low fiber contents. Mater Struct 2011;44:583–98.
[7] Orgass M, Klug Y. Fibre reinforced ultra-high strength concretes. In: International symposium on ultra-high performance concrete. 2004. p. 637–47.
[8] Naaman AE. New fiber technology. Cem Ceram Polym Compos 1998;1:57–62.
[9] Yoo DY, Kim S, Park GJ, Park JJ, Kim SW. Effects of fiber shape, aspect ratio, and volume fraction on flexural behavior of ultra-high-performance fiber-reinforced cement composites. Compos Struct 2017;174:375–88.
[10] Kim MJ, Kim S, Yoo DY. Hybrid effect of twisted steel and polyethylene fibers on the tensile performance of ultra-high-performance cementitious composites. Polymers 2018;10(8):879.
[11] Li VC, Wang S, Wu C. Tensile strain-hardening behavior or polyvinyl alcohol engineered cementitious composite (PVA-ECC). ACI Mater J 2001;98:483–92.
[12] Li VC, Wu C, Wang S, Ogawa A, Saito T. Interface tailoring for strain-hardening polyvinyl alcohol-engineered cementitious composite (PVA-ECC). ACI Mater J 2002;99:463–72.
[13] Pakravan HR, Jamshidi M, Latifi M. The effect of hydrophilic (polyvinyl alcohol) fiber content on the flexural behavior of engineered cementitious composites (ECC). J Text Inst 2018;109:79–84.
[14] Kong HJ, Bike SG, Li VC. Development of a self-consolidating engineered cementitious composite employing electrosteric dispersion/stabilization. Cem Concr Compos 2003;25:301–9.
[15] Ma J, Orgass M, Dehn F, Schmidt D, Tue NV. Comparative investigations on ultra-high performance concrete with or without coarse aggregates. In: International symposium on ultra-high performance concrete. 2004. p. 205–12.
[16] Collepardi S, Coppola L, Troli R, Collepardi M. Mechanical properties of modified reactive powder concrete. ACI Spec Publ 1997;173:1–22.
[17] ASTM C109-07. Standard test method for compressive strength of hydraulic-cement mortars. West Conshohocken, PA: ASTM International; 2008.
[18] ASTM C39-96. Standard test method for compressive strength of cylindrical concrete specimens. West Conshohocken, PA: ASTM International; 1998.
[19] JSCE. Recommendations for design and construction of ultra high performance fiber reinforced concrete structures. Tokyo, Japan: Japan Society of Civil Engineers; 2004 [draft].
[20] del Viso JR, Carmona JR, Ruiz G. Shape and size effects on the compressive strength of high-strength concrete. Cem Concr Res 2008;38:386–95.
[21] Hassan AMT, Jones SW, Mahmud GH. Experimental test methods to determine the uniaxial tensile and compressive behaviour of Ultra High Performance Fibre Reinforced Concrete (UHPFRC). Constr Build Mater 2012;37:874–82.
[22] Graybeal B, Davis M. Cylinder or cube strength testing of 80 to 200 MPa ultra-high-performance fiber-reinforced-concrete. ACI Mater J 2008;105:603–9.
[23] Kim MJ, Yoo DY, Kim S, Shin M, Banthia N. Effects of fiber geometry and cryogenic condition on mechanical properties of ultra-high-performance fiber-reinforced concrete. Cem Concr Res 2018;107:30–40.
[24] Yang E [PhD thesis] Designing added functions in engineered cementitious composites. MI: University of Michigan; 2008.
[25] Li VC, Leung CKY. Steady-State and Multiple Cracking of Short Random Fiber Composites. J Eng Mech 1992;118:2246–64.
[26] Naaman AE. Engineered steel fibers with optimal properties for reinforcement of cement composites. J Adv Concr Technol 2003;1:241–52.

[27] Wille K, El-Tawil S, Naaman AE. Properties of strain hardening ultra high performance fiber reinforced concrete (UHP-FRC) under direct tensile loading. Cem Concr Compos 2014;48:53–66.
[28] Yoo DY, Banthia N, Lee JY, Yoon YS. Effect of fiber geometric property on rate dependent flexural behavior of ultra-high-performance cementitious composite. Cem Concr Compos 2018;86:57–71.
[29] Li VC, Kanda T, Lin ZC. Influence of fiber/matrix interface properties on complementary energy and composite damage tolerance. Key Eng Mater 1998;145–149:465–72.
[30] Nehdi M, Ladanchuk JD. Fiber synergy in fiber-reinforced self-consolidating concrete. ACI Mater J 2004;101:508–17.
[31] Yao W, Li J, Wu K. Mechanical properties of hybrid fiber-reinforced concrete at low fiber volume fraction. Cem Concr Res 2003;33:27–30.